

Revisiting the Stimulation-Rate-Dependent Pattern Mismatch Negativity

Marc Pabst

Affiliation

Abstract

How does the brain process and represent successive sound in close temporal proximity? By investigating mismatch negativity (MMN) components, prior research (Sussman & Gumenyuk, 2005; Sussman, Ritter & Vaughan, 1998) has suggested that temporal proximity plays an important role in how sounds are represented in auditory memory. Here, we investigate how predictability affects the elicitation of mismatch negativity components in auditory sequences consisting of two tones (frequent tone A = 440 Hz, rare tone B = 494 Hz, fixed SOA 100 ms). In the predictable condition, tones are presented in a fixed order whereas in the unpredictable condition, standards and deviants are presented in a pseudo-random order. We expect to find that B tones in the unpredictable condition will elicit a significant MMN while B tones in the predictable conditions will not. A repeating five-tone pattern was presented at several stimulus rates (200, 400, 600, and 800 ms onset-to-onset) to determine at what temporal proximity the five-tone repeating unit would be represented in memory. The mismatch negativity component of event-related brain potentials was used to index how the sounds were organized in memory when participants had no task with the sounds. Only at the 200-ms onset-to-onset pace was the five-tone sequence unitized in memory. At presentation rates of 400 ms and above, the regularity (a different frequency tone occurred every fifth tone) was not detected and mismatch negativity was elicited by these tones in the sequence. The results show that temporal proximity plays a role in unitizing successive sounds in auditory memory. These results also suggest that global relationships between successive sounds are represented at the level of auditory cortices.

Revisiting the Stimulation-Rate-Dependent Pattern Mismatch Negativity

Abstract	2
Revisiting the Stimulation-Rate-Dependent Pattern Mismatch Negativity	3
Introduction	4
Methods and Materials	10
Participants	10
Procedure and Stimuli	10
Data Acquisition	11
Analysis Pipeline	12
Statistical Analysis	13
Results	15
Discussion	21

Introduction

Unraveling the mysteries of human perception might be one of the most fascinating and difficult challenges in cognitive sciences. We usually have little regard for this, but at every single moment, we achieve something outstanding: By forming a coherent representation from the tangled mess of external stimuli that reach our sensory organs, we make sense of the outside world. In doing so and seemingly effortlessly, we overcome complicated mathematical and philosophical problems. Recent advances in emerging fields like computer vision and machine hearing have provided a sense of how daunting these tasks can be—requiring complex models that consume vast amounts of computational resources and energy. What enables the brain to fulfill these functions with such ease while consuming no more than the power equivalent of a lightbulb?

Over the centuries, many theories have been broad forward in an attempt to answer these questions. While early philosophers like Aristotle believed in the idea of direct or naïve realism (the idea that the outside world is perceived directly), early modern scholars like John Locke promoted the concept of indirect realism, which is highly compatible with the assumption of representationalism in cognitive science (perceptual experiences result from an internal representation rather than directly from external objects). Among the first who developed a consistent theory defining the rules followed by indirect perception were the Gestalt psychologist of the early 20th century. Wertheimer, Koffka, and Köhler hypothesized that Gestalt principles, self-organizing rules on how individual elements should be grouped or separated, guide perception. They based their principle on the observation that humans perceive a global whole instead of just collections of individual parts.

Much later, auditory scientists faced the same challenges described in the first paragraph, but now in a very particular context: They were puzzled by the brain's ability to convert small air pressure fluctuations into actual auditory percepts. Somehow, the brain forms meaningful perceptual experiences from what can only be described as a busy mess of sound waves that originate from a plethora of different sources differing in pitch, loudness, and spatial position. Known as the *cocktail party effect* (Cherry, 1953), this problem was compared to inferring the

positions, shapes, and movements of motorboats on a lake—just by observing how two nearby objects move up and down the waves. Attempts to find answers to this perplexing question lead to the development of auditory scene analysis (ASA). Not unlike the concepts proposed by the Gestalt theorists six decades earlier, (Bregman, 1990) suggested that the brain uses so-called *streaming* and *segregation* to form auditory objects from rich spectro-temporal information. At its core, ASA relies on two different categories of grouping, namely *sequential* and *simultaneous* integration: Simultaneous integration (or vertical integration) refers to the grouping of concurrent properties into one or more separable auditory objects, a process informed by temporal cues like common onset and offset, spectral and spatial characteristics. Sequential integration (or horizontal integration), on the other hand, describes how temporally distinct sounds are merged into one or multiple coherently perceived streams (contrary to auditory objects in simultaneous grouping, only one such stream can be actively perceived at any time). While vertical and horizontal grouping can come to different and therefore competing results, sequential grouping often takes precedence over cues for simultaneous integration (Bendixen, 2014)

As is so often the case, the key to understanding such complex phenomena seems to lie in learning about the most basic processing steps. In auditory research, these steps usually come in the shape of very simple stimuli, often consisting of nothing more than pure tones. Such stimuli were also the first to be used in the auditory oddball paradigm, a now well-established and robust paradigm extensively used in event-related potential (ERP) studies (Squires et al., 1975). In its basic form, participants are presented with a series of similar tones or sounds (so-called *standard* events), interrupted by rare tones or sounds that differ in at least one feature (*deviant* events) from the more frequent ones. Strikingly, deviant events elicit more extensive neural activity over sensory areas. This finding is known as the mismatch negativity (MMN) component because when measured using EEG, a robust negative deflection can be observed in the difference wave obtained by subtracting the response to deviant events from the response to standard events. Negativity is strongest in the frontotemporal area of the scalp, with a peak latency ranging from 100 to 250 ms after stimulus onset. The elicitation of an MMN is not restricted to the repetition of physically identical stimuli but can also be observed when deviant events are complex, e.g.,

when abstract auditory regularities are violated (Paavilainen, 2013). The regularities can come in the form of relationships between two tones (Saarinen et al., 1992) or multiple tones (Alain et al., 1994; Nordby et al., 1988; Schröger et al., 1996).

Interestingly, this finding is also highly compatible with another prevalent theory of perception, namely the idea that perception is not (only) a stimulus-driven bottom-up process, but is informed by internal predictions of some kind. These kinds of ideas have been around a long time and famously trace back to the physiologist Hermann von Helmholtz but were also proposed by numerous other scientists such as Richard Gregory. Most recently, this notion has been introduced in a theory known as (hierarchical) predictive coding. Predictive coding specifically suggests that at every processing state, predictions from so-called *probabilistic generative models* and sensory input are compared continuously, and only their difference, termed *prediction error*, is propagated. MMN responses have been proposed as an index of prediction error (Wacongne et al., 2011). Although other interpretations exist (e.g., May & Tiitinen, 2010), the MMN is frequently interpreted as a marker of expectation violations stressing the role predictions play in perception (e.g., István Winkler, 2007).

An interesting situation arises when concurrent predictive clues exist. Following this idea, E. Sussman et al. (1998) presented participants with a sequence of frequent pure tones and rare pitch deviants while reading a book of their choice. Tones were arranged in a predictable five-tone pattern consisting of four standard tones and one deviant (i.e., A-A-A-A-B-A-A-A-B, ‘-?’ indicating silence between the tones). ERPs to A and B tones were compared for rapid (SOA of 100 ms) and slow (SOA of 1200 ms) stimulation rates. The 100 ms SOA condition also included a control condition in which tone order was pseudo-randomized (e.g., A-A-A-B-A-B-A-A-A) without altering deviant probability ($p_B = .20$). When tones are presented randomly, only their relative frequency of occurrence carries value for predicting the pitch of the next tone. This, we refer to as *proportional regularity*. However, in an ordered presentation, a sequence of four standard tones is always followed by one deviant tone. Thus, understanding this relationship should allow for *perfect prediction* in which all deviant tones are expected with near-absolute certainty. We call this regularity a *pattern regularity*. Provided the underlying

mechanism can incorporate such information, the processing of the pitch deviants should correspond with that of standard tones, and therefore no MMN would be elicited. Interestingly, in the case of Sussman et al., MMNs were only elicited if tone presentation was slow and predictable or fast and random, but not when predictable tones were presented rapidly. In a subsequent study, E. S. Sussman & Gumenyuk (2005) used the same pattern at different SOAs (200 ms, 400 ms, and 800 ms). Similar to their previous study, ordered presentation at 400 ms and 800 ms SOA elicited an MMN response, while at a stimulation rate of 200 ms, evidence for such a deflection was absent. Sussman et al. attributed this observation to sensory memory limitations. That is, only when auditory memory can accommodate enough repetitions of the five-tone pattern; the brain can integrate tones into a coherent representation allowing for accurate predictions of deviant tones. This, in turn, would explain the absence of MMNs in the fast presentation condition. Based on this, they argued that while true for fast presentation rates with SOAs up to 200 ms, for longer SOAs, pattern durations would be too long, and thus representations would exceed sensory memory capacity.

In a recent in-class replication study, Scharf & Müller (in prep) presented participants with the same stimuli as Sussmann in a very similar experimental setting. Their study only differed in that participants were given a simple task in which they had to count visual targets instead of reading a book of their choice. Surprisingly, while descriptive results were compatible with those of Sussmann et al., pairwise comparisons revealed no significant effect when comparing deviant and standard tones for both the *random* and the *predictable* condition. Further Bayesian analysis remained largely inconclusive, providing only *anecdotal* evidence in favor of such an effect for *random* presentation and *moderate* evidence for its absence in the *predictable* condition. In the face of the replication crisis, many scientists have become painfully aware of the importance of replicability (Ioannidis, 2005). Exact or quasi-exact replication studies that try to match the original study's experimental conditions as closely as possible are regarded as the gold standard of science (Jasny et al., 2011; Popper, 1935). However, replications that extend, change, or optimize materials or methods of the original work also offer valuable insight. This kind of replication is known as conceptual (Schmidt, 2009) and refers to using of different methods to repeat the test of a hypothesis or experimental result.

This thesis seeks to replicate the findings by Sussman et al. It largely follows the procedure laid out by E. S. Sussman & Gumenyuk (2005). However, it deviates from the original design in some critical aspects. First, the aforementioned five-tone patterns are presented in both the *predictable* condition and in the *random* context. That is, pseudo-random order will be deliberately broken by occasionally presenting B-A-A-A-A-B-patterns. In particular, this will ensure that the local history of B-tones in the *random* condition is comparable to that in the *predictable* condition. Secondly, B tones are compared exclusively with their preceding A tones. Lastly, a small number of A-A-A-A-B will be replaced by A-A-A-A-A sequences in both conditions, allowing the comparison of physically identical tones in different contexts. The advantages of this design are discussed in more detail in the following paragraphs. A pre-registration covering data collection, processing, and analysis is available at <https://osf.io/cg2zd/>. Deviations from this pre-specified plan and further exploratory analyses are explicitly reported.

E. S. Sussman & Gumenyuk (2005) interpretation of the original results suggests that at fast stimulation rates (200 ms and faster), pattern-based regularities take precedence over proportion-based regularities. If this is indeed true, B-tones in the *predictable* condition should not be considered a *mismatch* and thus should not elicit an MMN response. In contrast, since there is no way to reliably predict B-tones in the *random* condition, these tones would still be considered *deviant* events and are therefore expected to generate an MMN. On the other hand, when an A tone replaces a predictable B tone, one would expect an MMN, despite tones are physically identical. Specifically, hypotheses are formulated in regards to the ERPs elicited by the 5th tone in the five-tone sequence (A-A-A-A-**B** or A-A-A-A-**A**; boldface marks tone of interest) compared to the 4th tone in that sequence (A-A-A-A-X, ?X? marking either an A or an B tone). Hypotheses can be summarized as follows:

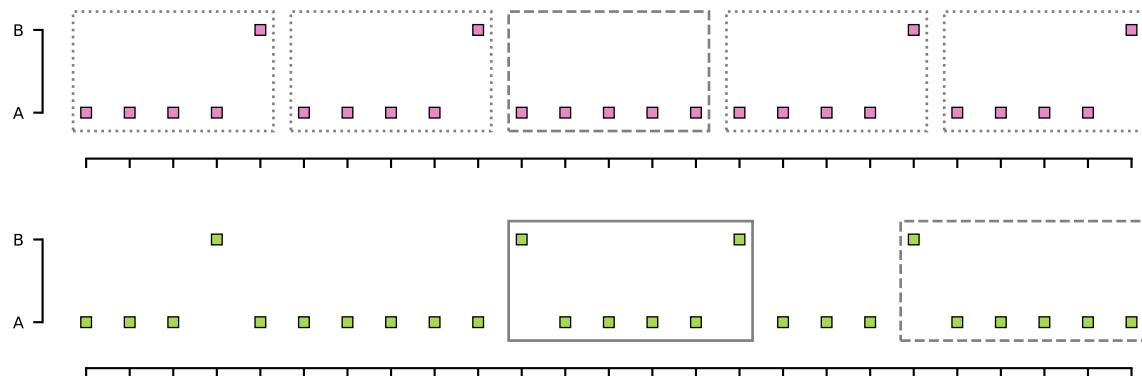
Pattern regularities If Sussman's interpretation holds, one expects i) negativity in the N1/MMN time domain (about 100-200 ms after tone onset) for deviations in the BAAAAB sequence in the *random* condition, since B tones violate the *proportional regularity*, ii) one expects no evidence for such an effect (or evidence favoring \mathcal{H}_0 i.e., that there is no effect) in the

predictable context since more informative higher-order predictions based on *pattern regularity* are not violated, and iii) the difference waves should differ significantly. Also, the comparison between the 5th A tone and the proceeding A tone (A-A-A-A-X vs. A-A-A-A-A) should be considered a *mismatch* and is therefore expected to elicit a significant MMN response.

Proportional regularities If, however, no *pattern regularity* is extracted, B-tones should continuously result in an MMN regardless of presentation context since the predictive value of the *proportional regularity* does not differ between conditions. When presenting A tones at the 5th position, no MMN should occur. Also, difference waves should not differ.

Pattern regularities and proportional regularities As a third possibility, the brain might use *proportional regularities* and *pattern regularities* concurrently, resulting in negativity following B-tones in either condition. Fifth-position A tones should constitute an expectation violation and should therefore result in a negative deflection.

FIGURE 1.

Caption

Methods and Materials

Participants

All participants were recruited at the Institute of Psychology at the University of Leipzig and reported good general health, normal hearing, and had a normal or corrected-to-normal vision. Written informed consent was obtained before the experiment. Participants were blinded to the purpose of the experiment and were compensated in course credit or money.

100 ms Presentation Rate Data were collected from twenty participants (2 males, average age 22.3 yrs., $SD = 6.46$, range 18 - 41 yrs.).

150 ms Presentation Rate The sample consisted of twenty-three psychology undergraduate students (2 males, average age 22.6 yrs., $SD = 5.57$, range 18 - 42).

Procedure and Stimuli

Participants sat in a comfortable chair in a sound-insulated chamber. The experimental setup was practically identical to that of Sussman et al.; however, instead of reading a book, subjects were asked to direct their attention to a self-selected movie. Movies were presented with subtitles but without sound. Commercially available software (MATLAB R2014a; The MathWorks Inc, Natick, MA) in conjunction with the Psychophysics Toolbox extension (version

3.0.12, Brainard, 1997; Kleiner et al., 2007) was used to control stimulus presentation. Stimuli consisted of pure sinusoidal tones with a duration of 50 ms (including a 10 ms cosine on/off ramp), presented isochronously at a stimulation onsets asynchrony (SOA) of 100 ms and 150 ms, respectively. Blocks contained 820 frequent 440 Hz tones (‘A’ tones) and 120 infrequent 449 Hz tones (‘B’ tones), delivered binaurally using Sennheiser HD-25-1 II headphones at 70 dB. For the 100 ms condition, participants were presented with 40 blocks (100 s duration each), while 20 blocks (150 s duration) were presented in the 150 ms condition. In one-half of the blocks, tones occurred in pseudo-random order (e.g., A-A-A-B-A-B-A), *random* condition) while in the other half, tone presentation followed a simple pattern in which a five-tone-sequence of four frequent tones and one infrequent tone (i.e., A-A-A-A-B) was repeated cyclically (*predictable* condition). Block order was counterbalanced across participants. Additionally, A tones replaced 10% of designated (infrequent) B tones, resulting in sporadic five-tone sequences consisting solely of A tones (i.e., A-A-A-A-A), thus violating the *pattern regularity*. Care was taken that sequences in the *random condition* were always separated by at least five pseudo-random tones and that A-A-A-A-A-patterns were always separated by at least two A-A-A-A-B-patterns. To assure comparability of local histories between tones of interest in both conditions, pseudo-randomly arranged tones were interspersed with sequences matching those from the predictable condition (B-A-A-A-A-B and B-A-A-A-A-A). A total of 2000 tones at 150 ms SOA or 4000 tones at 100 ms SOA were delivered to each participant.

Data Acquisition

Electrophysiological data were recorded from active silver-silver-chloride (Ag-AgCl) electrodes using an ActiveTwo amplifier system (BioSemi B.V., Amsterdam, The Netherlands). A total of 39 channels were obtained using a 32-electrode-cap and seven external electrodes. Scalp electrode locations conformed to the international 10–20 system. Horizontal and vertical eye movement was obtained using two bipolar configurations with electrodes placed around the lateral canthi of the eyes as well as above and below the right eye. Additionally, three electrodes were placed on the tip of the nose and at the left and right mastoid sites. Data were sampled at 512 Hz and on-line low-pass filtered at 1000 Hz.

Analysis Pipeline

Data preprocessing was implemented using a custom pipeline based on the *MNE Python* software package (Gramfort, 2013) using *Python 3.7*. All computations were carried out on a cluster operated by the University Computation Center of the University of Leipzig. Code used in this thesis is publicly available at <https://github.com/marcpabst/xmas-oddballmatch>.

First, EEG data were subjected to the ZapLine procedure (de Cheveigné, 2020) to remove line noise contamination. A fivefold detection procedure, as described by Bigdely-Shamlo et al. (2015) was then used to detect and subsequently interpolate bad channels. Namely, this included detecting channels that contained prolonged segments with very small values (i.e., flat channels), the exclusion of channels based on robust standard deviation (deviation criterion), unusually pronounced high-frequency noise (noisiness criterion), and the removal of channels that were poorly predicted by nearby channels (correlation criterion and predictability criterion). Channels considered bad by one or more of these methods were removed and interpolated using spherical splines (Perrin et al., 1989). Electrode locations for interpolations were informed by the BESA Spherical Head Model.

For independent component analysis (ICA), a 1-Hz-high-pass filter (134th order hamming-windowed FIR) was applied (Irene Winkler et al., 2015). Artifact Subspace Reconstruction (ASR, Mullen et al., 2015) was used to identify and remove parts of the data with unusual noise characteristics (bursts). ICA was then carried out using the *Picard* algorithm (Ablin et al., 2018, 2017) on principal-component-analysis-whitened (PCA) data. PCA was also used for dimensionality reduction to avoid rank-deficiency when extracting components from data with one or more interpolated channels. The EEGLAB (version 2020.0, Delorme & Makeig, 2004) software package and the IClab plugin (version 1.2.6, Pion-Tonachini et al., 2019) were used to classify estimated components automatically. Only components clearly classified (i.e., confidence above 50%) resulting from either eye movement, muscular, or heartbeat activity were zeroed-out before applying the mixing matrix to unfiltered data. It should be noted that this procedure deviated from the pre-registration in that it was fully automated.

In line with recommendations from Widmann et al. (2015) and de Cheveigné & Nelken (2019), a finite impulse response (FIR) bandpass filter from 0.1 Hz to 40 Hz (Hamming window, 0.1 Hz lower bandwidth, 5 Hz upper bandwidth, 0.0194 passband ripple, and 53 dB stopband attenuation). Continuous data were epoched into 400 ms long segments around stimulus onsets, including a 100 ms pre-stimulus interval. No baseline correction was applied, and segments exceeding a peak-to-peak voltage difference of 100 μ V were removed. On average, 45 epochs were dropped. No dataset met the pre-registered exclusion criterion of less than 100 valid trials per condition; thus, data from all participants (20 for 100 ms presentation rate and 23 for 150 ms presentation rate) were analyzed.

Statistical Analysis

Statistical analysis was carried out using the *R* programming language (version 3.2, The R Core Team) using the *rstatix* package (version 2.0, Kassambara, 2020).

Calculation of the dependant variable followed the original study's procedure in averaging amplitudes in a time window extending ± 25 ms around the expected peak of negativity. Specifically, this peak was obtained by subtracting the average ERP following the A tones from the average ERP following B tones in the *random condition* for both presentation rates separately. To compute mean amplitudes, ERPs to 4th position A tones (A-A-A-A-X, **boldface** indicates the tone of interest) and B tones (A-A-A-A-B) were averaged separately for both the *random* and the *predictable condition*. For the *random condition*, only tones presented as part of a sequence matching the patterns from the *predictable condition* were included in the analysis.

In accordance with the original analysis by E. S. Sussman & Gumenyuk (2005), mean amplitudes for frontocentral electrodes (pooled FZ, F3, F4, FC1, and FC2) and the two mastoid positions (pooled M1 and M2) were averaged separately. Then, for both SOAs, independent two-way repeated-measures analyses of variance (ANOVA) with factors *condition* (levels *predictable* and *random*), *stimulus type* (levels *A tone* and *B tone*), *electrode locations* (levels *frontocentral* and *mastoids*), and all possible interactions were calculated. Following this, significant interaction effects were further investigated using post-hoc *t*-tests.

Going beyond the original study and extending the pre-registered procedure, Bayesian analysis was conducted for ANOVA posthoc comparisons. As mentioned above, traditional null hypothesis testing has some limitations that are often overlooked, leading to incorrect conclusions drawn from results. For example, not rejecting the null hypothesis can usually not be interpreted as evidence in favor of \mathcal{H}_0 (e.g., Aczel et al., 2018; Goodman, 2008; Kirk, 1996; Meehl, 1978). Similarly, p-values might exaggerate evidence against \mathcal{H}_0 (that is, observed data might be more likely under \mathcal{H}_0 than under \mathcal{H}_1 even though \mathcal{H}_0 is rejected, e.g., Hubbard & Lindsay, 2008; Rouder et al., 2009; Sellke et al., 2001; Wagenmakers et al., 2018). Conversely, Bayesian hypothesis testing using Bayes factors can provide an intuitive way to compare observed data's likelihood under the null hypothesis versus the alternative hypothesis (Wagenmakers, 2007), thereby making it possible to evaluate the null hypothesis as well:

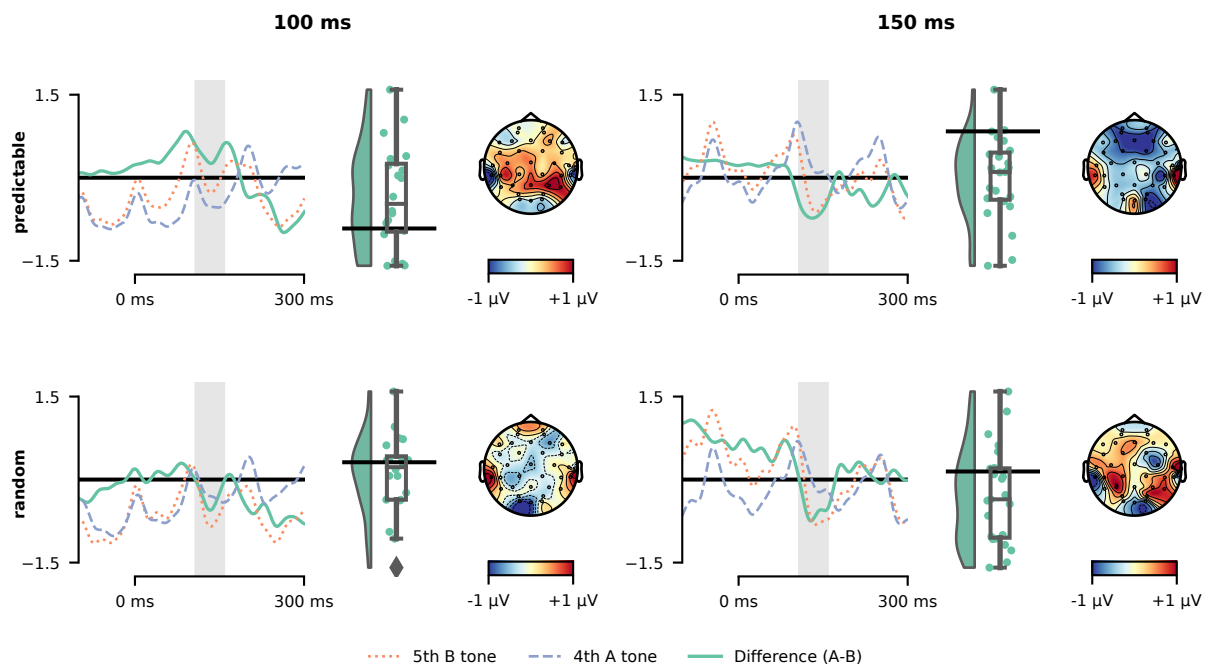
$BF_{10} = \frac{Pr(data|\mathcal{H}_0)}{Pr(data|\mathcal{H}_1)}$. Here, this approach was applied in agreement with the concept described by Rouder et al. (2009) as an alternative to classical frequentist paired t -tests. Following this sentiment, Bayes factors for within-participant differences y_i were computed assuming $\mathcal{H}_0 : y_i \sim Normal(0, \sigma^2)$ and $\mathcal{H}_1 : y_i \sim Normal(\delta, \sigma^2)$; $\delta \sim Cauchy(0, 1/\sqrt{2})$. A Jeffreys prior was used for the variance σ^2 in both models: $p(\sigma^2) \propto 1/\sigma^2$. Calculations were performed using the Hamiltonian Monte Carlo method implemented in *Stan* (version 2.25, Carpenter et al., 2017) and *RStan* (Stan Development Team, 2020).

Finally, the relationship between epoch number and the reliability analysis was analyzed by drawing random subsamples of different sizes from both data sets and calculating split-half reliability employing the Spearman–Brown approach. Thus, single-trial responses for all A and B tones in the predictable condition were randomly shuffled. Then, 100, 200, ..., N_{max} ($N_{max,100ms} = 3000$, $N_{max,150ms} = 1500$) epochs were drawn, randomly assigned to one of two halves, and averaged separately for A and B tones. Then, split-half reliability was calculated using the differences between A and B tones in the MMN latency window using the Spearman–Brown prophecy formula¹ (Brown, 1910; Spearman, 1910). This procedure was repeated 100 times for each N , and split-half-reliabilities obtained were subsequently averaged.

¹ as given by $\rho_{xx'} = \frac{2\rho_{12}}{1+\rho_{12}}$, where ρ_{12} is the Pearson correlation coefficient between the two halves.

FIGURE 2.

ERP grand averages (pooled FZ, F3, F4, FC1, and FC2 electrode locations) for an SOA of 100 ms (left) and 150 ms (right), for A tones (A-A-A-A-X, blue dashed lines) and B tones (A-A-A-A-B, orange dashed line) and their difference (B - A, green solid line). Upper panels show ERPs for tones presented in a predictable pattern (predictable condition) while lower panels show ERPs for tones presented in pseudo-random order (random condition). Shaded area marks MMN latency window (110 ms to 160 ms) used to calculate the distribution of amplitude differences across participants (middle of each panel) and the difference of topographic maps averaged over the same interval (right of each panel).

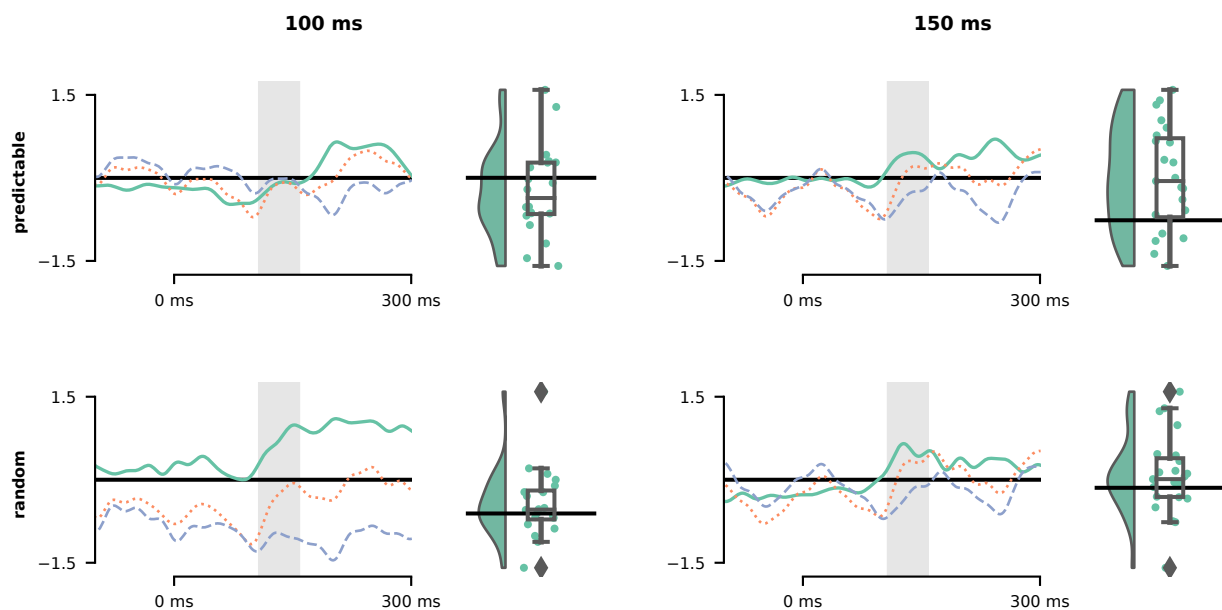


Results

Fig. 2 displays grand averages of event-related potentials (ERP) at pooled FZ, F3, F4, FC1, and FC2 electrode locations to A tones (A-A-A-A-X), B tones (A-A-A-A-B), and their difference (B tone minus A tone) for both 100 ms (left panel) and 150 ms (right panel) SOAs. The top half of each panel shows ERPs in the *predictable condition* while the lower half depicts ERPs in the *random condition*. Clearly visible rhythms result from fast presentation frequencies and illustrate the considerable overlap between neighboring tones. Panels also show the distribution of mean amplitude differences in the MMN latency window across participants and the difference of scalp topographies. Similarly, waveforms and mean amplitude difference distributions at pooled

FIGURE 3.

ERP grand averages (pooled M1, M2 electrode locations) for an SOA of 100 ms (left) and 150 ms (right), for A tones (A-A-A-A-X, blue dashed lines) and B tones (A-A-A-A-B, orange dashed line) and their difference (B - A, green solid line). Upper panels show ERPs for tones presented in a predictable pattern (predictable condition) while lower panels show ERPs for tones presented in pseudo-random order (random condition). Shaded area marks MMN latency window (110 ms to 160 ms) used to calculate the distribution of amplitude differences across participants.



mastoid sites are shown in fig. 3.

The MMN latency window was determined to range from 108 ms to 158 ms after stimulus onset for 100 ms SOA and from 104 ms to 154 ms after stimulus onset for 150 ms SOA. Mean amplitudes from that interval are shown in Table 1. Descriptively, mean amplitudes at pooled frontocentral electrode locations were more negative for randomly presented B tones than for randomly presented A tones, regardless of presentation rate (100 ms: $\Delta M = -0.361 \mu V$; 150 ms: $\Delta M = -0.518 \mu V$). A similar observation could be made for predictable tones presented at 150 ms SOA ($\Delta M = -0.588 \mu V$). Strikingly however, when presented at 100 ms SOA, B tones seemed to elicit more positive responses than A tones ($\Delta M = 0.379 \mu V$).

Statistical analysis was carried out using independent two-way repeated-measures analysis of variance (ANOVA, Table 2). For the 100 ms SOA presentation, ANOVA results for the

frontocentral electrode cluster revealed a significant effect of the interaction term (*condition x stimulus type*; $F(1, 19) = 17.00, p = 0.0006$). For slower tone presentation ($SOA = 150ms$), ANOVA results suggested a main effect of factor *stimulus type* for both frontocentral ($F(1, 22) = 21.62, p < .001$) and mastoid electrodes ($F(1, 22) = 6.26, p = 0.0200$). ANOVAs for the comparison between the 4th A tone and the 5th A tone (A-A-A-A-X versus A-A-A-A-A; Table 2) did not result in any significant effects.

Table 1

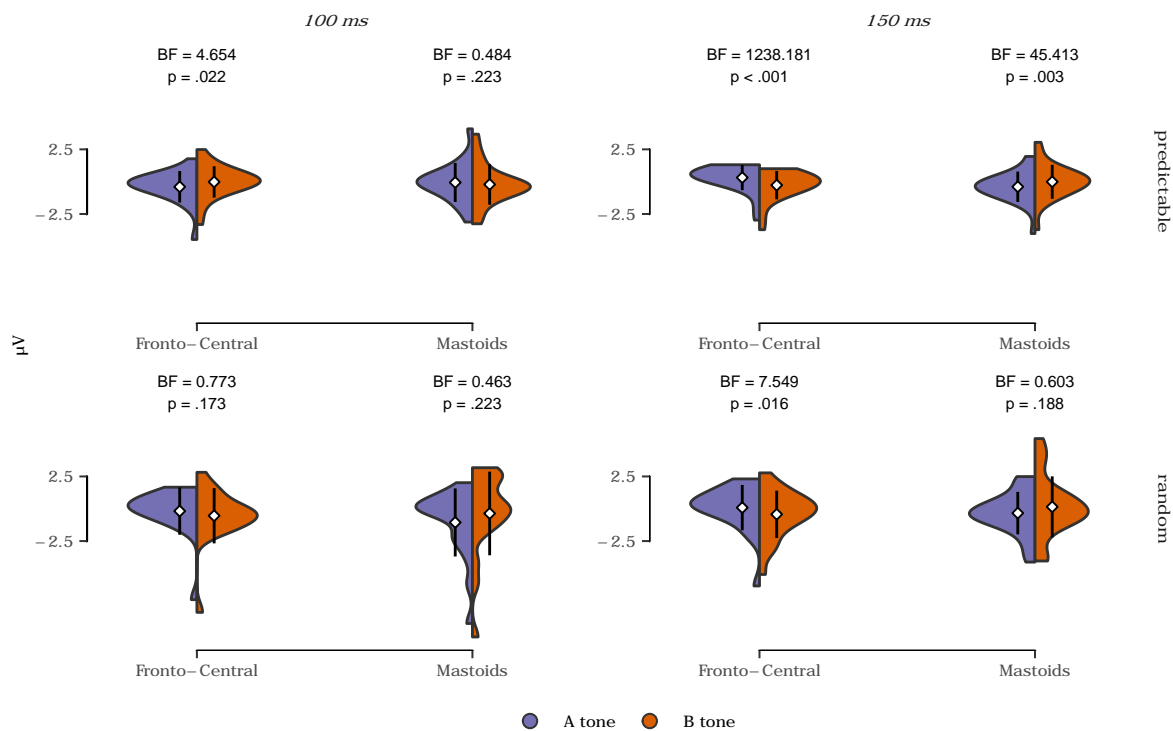
Results of the 2-way ANOVA (condition x stimulus type) for repeated measures. Only fronto included.

		Effect	DFn	DFd	F	p	p<.05	ges
100 ms	Frontal	Condition	1	19	0.137	.715		0.002
		StimulusType	1	19	0.004	.953		8.21e-06
		Condition x StimulusType	1	19	17	< .001	*	0.013
	Mastoids	Condition	1	19	1.39	.253		0.015
		StimulusType	1	19	0.946	.343		0.003
		Condition x StimulusType	1	19	2.2	.154		0.008
150 ms	Frontal	Condition	1	22	0.775	.388		0.005
		StimulusType	1	22	21.6	< .001	*	0.036
		Condition x StimulusType	1	22	0.194	.664		0.000147
	Mastoids	Condition	1	22	0.187	.670		0.001
		StimulusType	1	22	6.26	.020	*	0.017
		Condition x StimulusType	1	22	0.102	.753		0.000236

Significant interactions indicate that difference waves between A and B tones differ across conditions. Two-tailed Student's *t*-tests and complementary Bayesian analysis were used to test individual MMN responses for significance from zero. P-values were corrected for multiple comparisons using the Benjamini–Hochberg step-up procedure. Results indicate that responses to B tones are more positive in comparisons to A tones when presented in a predictable context ($t(19) = -2.81, p = .022, CI_{.95} = [-0.66, -0.10], BF_{10} = 4.65$). Although

FIGURE 4.

Averaged voltages in the MMN latency window for pooled frontocentral and mastoid electrodes. Colored areas show sample probability density function for A tones (green) and B tones (red). White diamonds indicate estimated population mean, vertical bars represent 95%-confidence interval. Only Benjamini-Hochberg-corrected p -values < 0.05 are shown.



descriptive statistics indicated a contrary effect for randomly tones presented, results remained inconclusive ($t(19) = 1.69, p = .173, CI_{.95} = [-0.09, 0.81], BF_{10} = 0.77$).

To investigate whether absence of evidence for an MMN might be due to low within-participant sample sizes, the analysis was repeated for the *random* condition including not only B tone trials that occurred within a five-tone sequence (as with the pre-registered analysis path), but all B tones and their immediately preceding A tone. Results from this comparison are shown in (Fig?):??.

Split-half reliabilities are displayed in fig. 6. Simulated values match the curve expected from the Spearman-Brown formula. In the context of classical test theory, this method relates the length of a test (or *experiment*) to the number of items (or *trials*). The first derivative of the Spearman-Brown function is monotonically decreasing, leading to two different observations: i)

FIGURE 5.

ERP grand averages (pooled FZ, F3, F4, FC1, and FC2 electrode locations) for an SOA of 100 ms (left) and 150 ms (right), for 4th A tones (A-A-A-X, blue dashed lines) and 5th A tones (A-A-A-A-A, orange dashed line) and their difference (B - A, green solid line). Upper panels show ERPs for tones presented in a predictable pattern (predictable condition) while lower panels show ERPs for tones presented in pseudo-random order (random condition). Shaded area marks MMN latency window (110 ms to 160 ms) used to calculate the distribution of amplitude differences across participants (middle of each panel) and the difference of topographic maps averaged over the same interval (right of each panel).

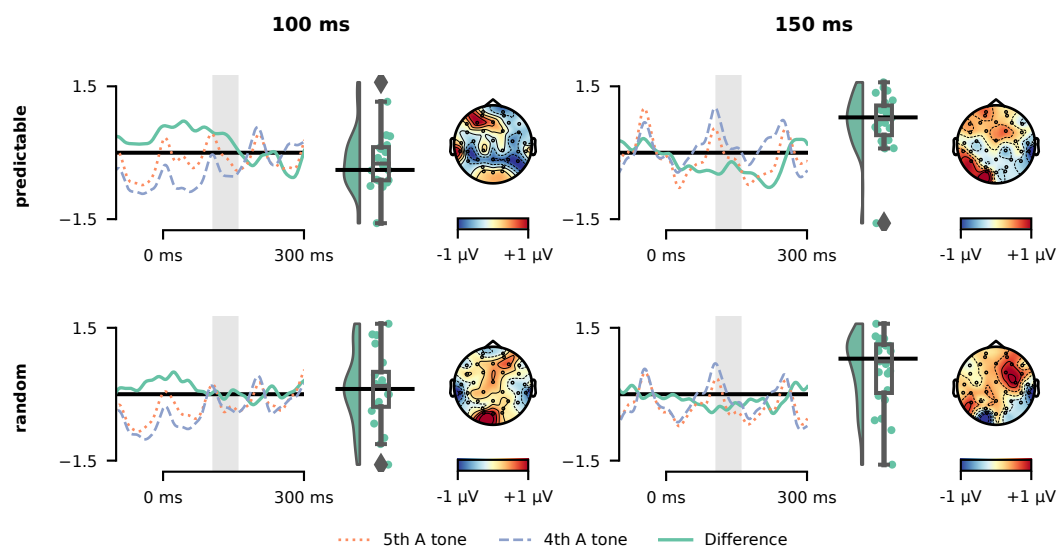


FIGURE 6.

EEG waveforms for five-tone sequences presented in an predictable context (dotted line) and pseudo-random condition (dashed line) for 100 ms presentation rate (top panel) and 150 ms presentation rate (lower panel). Vertical lines indicate tone onset.

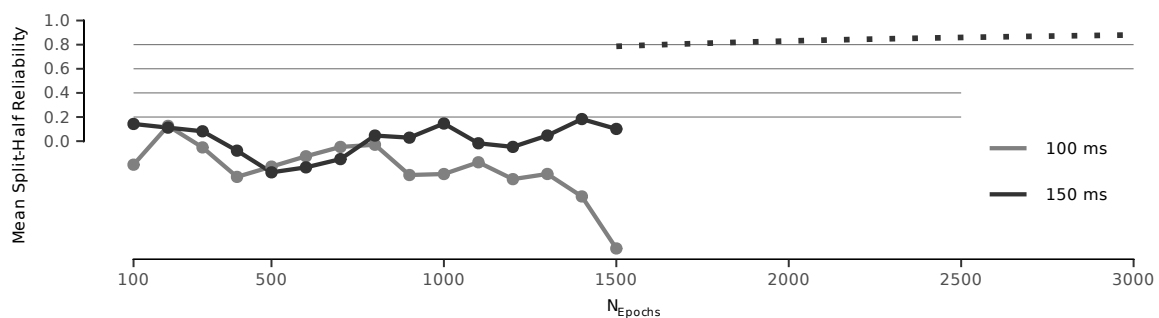


Table 2

Results of the 2-way ANOVA (condition x stimulus type) for repeated measures. Only fronto included.

		Effect	DFn	DFd	F	p	p<.05	ges
100 ms	Frontal	Condition	1	19	0.026	.873		0.000441
		StimulusType	1	19	0.938	.345		0.002
		Condition x StimulusType	1	19	0.961	.339		0.002
	Mastoids	Condition	1	19	3.59	.073		0.063
		StimulusType	1	19	1	.330		0.003
		Condition x StimulusType	1	19	0.822	.376		0.005
150 ms	Frontal	Condition	1	22	0.938	.343		0.003
		StimulusType	1	22	1.6	.219		0.008
		Condition x StimulusType	1	22	0.074	.789		0.000258
	Mastoids	Condition	1	22	0.875	.360		0.005
		StimulusType	1	22	2.8	.109		0.009
		Condition x StimulusType	1	22	0.93	.345		0.003

Adding additional epochs (extending the test length by an absolute value in classical test theory terms) has a large effect when the number of already present epochs is low, but has only little effect when already dealing with large numbers of epochs and ii) SOA and thus effect sizes have a larger impact when epoch numbers are small compared to high epoch numbers. Graphed values also show that reliabilities for the 100 ms stimulation rate are considerably lower than for an SOA of 150 ms and that reliabilities are very low when using a relatively small number of epochs. There is no generally accepted rule as to the level above which the coefficient can be considered acceptable. Rather, reliability should be evaluated based on the purpose of a study considering the cost-benefit trade-off (Nunnally et al., 1994). As laid out, increased reliability comes at overproportionate cost, in that collecting more samples will not increase reliability by the same factor. That said, many published articles deem reliability coefficients above .7 or .8 acceptable? (Lance et al., 2006).

Discussion

For the 150 presentation, extreme evidence for an MMN and very strong evidence for an accopying polarity reversal at the mastoids was found in the *predcitable* condition, that is, when tones were presented in a repeated five-tone pattern. When tones were presented in random order, strong evidence was foun[[anova_02_100_posthoc]] anova_02_100_posthoc.texd for an MMN but Bayes factors suggested inconclusive evidence for mastoids. In light of the resuts by E. S. Sussman & Gumenyuk (2005), we would

We found strong evidence for an MMN in the 150 ms delivery rate condition when comparing standards and deviants, regardless of the type of presentation (predictable vs. random). This finding is incompatible with the results and intepretation by (E. S. Sussman & Gumenyuk, 2005) but suggests that *pattern regularities* do not inform prediction. Furthermore, no convincing evidence for an MMN was found when comparing the 4th standard to the 5th standard in predictable condition.

For the 150 ms , significant MMN componets were found regardless of presentation

Lorem ipsum dolor sit amet, consectetur adipiscing elit. Donec id cursus velit, non egestas quam. Aliquam rutrum eget sem ut aliquet. Etiam euismod purus et gravida volutpat.

	random context	predictable context		difference wave
Intepretation	$\mathcal{H}_1 : B_{5th} < A_{4th}$	$\mathcal{H}_1 : B_{5th} < A_{4th}$	$\mathcal{H}_1 : A_{5th} < A_{4th}$	$\mathcal{H}_1 : \Lambda_{rand} \neq \Lambda_{pred}$
<i>pattern regularities</i>	×	✓	✓	✓
<i>proportional regularities</i>	✓	✓	×	×
<i>pattern regularities and proportional regularities</i>	✓	✓	✓	~
Results: 100 ms	×	inc.	inc.	✓
Results: 150 ms	✓	✓	inc.	inc.

✓: \mathcal{H}_1 is true / \mathcal{H}_0 rejected, ×: \mathcal{H}_0 is true, inc: inconclusive results ~: no explicit expectation

Suspendisse consequat ipsum nibh, vitae convallis dolor efficitur a. Suspendisse vehicula erat posuere velit fermentum viverra. Proin sapien urna, iaculis ut ultricies ac, auctor eu est. Nunc ornare pharetra finibus. Morbi finibus, ipsum non accumsan cursus, metus nisl egestas leo, et aliquam nisi leo quis diam. Quisque id diam non risus elementum convallis. Duis non nisl at nisl imperdiet vestibulum. Suspendisse efficitur porttitor nulla a vehicula. Interdum et malesuada fames ac ante ipsum primis in faucibus. Praesent tempor urna in orci congue, non euismod eros volutpat. Integer ullamcorper auctor libero, in laoreet nulla hendrerit ultrices.

Proin malesuada nisi et luctus volutpat. Nam ac posuere enim. Proin nec augue tincidunt felis ullamcorper luctus ac sit amet mi. Maecenas aliquam leo quis enim gravida maximus. Sed nec pellentesque magna. Vivamus et purus lacus. Donec maximus purus at fermentum efficitur. Phasellus auctor orci sem, eu sollicitudin eros pretium a.

In maximus libero at purus lobortis efficitur. Aliquam nec sapien consequat, lobortis lorem id, luctus velit. Pellentesque habitant morbi tristique senectus et netus et malesuada fames ac turpis egestas. Vestibulum dictum ipsum eu nunc maximus, quis ornare augue tincidunt. Nam leo purus, mollis quis nunc sed, sagittis tempus orci. In condimentum et neque ut laoreet. Curabitur accumsan ligula eu libero iaculis ullamcorper. Interdum et malesuada fames ac ante ipsum primis in faucibus. Nullam iaculis tellus risus, vitae dapibus augue commodo a. Sed ante dolor, fermentum at lectus id, pulvinar viverra elit. Aenean tincidunt mollis imperdiet.

Nulla id molestie neque, vitae vulputate velit. Fusce a velit imperdiet felis porttitor scelerisque. Nam tempus tincidunt elit, id finibus tortor tristique non. Ut imperdiet finibus mauris, in fringilla mauris blandit auctor. Etiam volutpat quam et feugiat elementum. Duis finibus fermentum condimentum. Donec sollicitudin molestie dolor. Cras convallis lorem orci, ut sagittis risus rutrum eget. Donec vel lobortis justo.

Pellentesque habitant morbi tristique senectus et netus et malesuada fames ac turpis egestas. Proin non leo vehicula, congue elit faucibus, tincidunt diam. Sed euismod vulputate mauris. Duis dapibus faucibus arcu, ut vehicula tellus blandit eu. Duis erat magna, cursus quis urna nec, placerat blandit lectus. Maecenas dolor quam, pharetra a urna eu, mollis iaculis dolor.

Aliquam maximus ante eget felis faucibus porta. Cras semper felis non tellus rutrum tempus. Morbi quam metus, volutpat nec aliquam at, interdum a nibh. Sed hendrerit purus tempor ex placerat, ut fringilla nulla molestie. Nullam vitae sem non purus lobortis fermentum. Quisque ligula tellus, ullamcorper sit amet consectetur quis, fermentum ac mi. Nunc pretium mollis dictum.

References

- Ablin, P., Cardoso, J.-F., & Gramfort, A. (2018). Faster independent component analysis by preconditioning with Hessian approximations. *IEEE Transactions on Signal Processing*, 66(15), 4040–4049. <https://doi.org/10.1109/TSP.2018.2844203>
- Ablin, P., Cardoso, J.-F., & Gramfort, A. (2017). Faster ICA under orthogonal constraint. *arXiv:1711.10873 [Stat]*. <http://arxiv.org/abs/1711.10873>
- Aczel, B., Palfi, B., Szollosi, A., Kovacs, M., Szaszi, B., Szecsi, P., Zrubka, M., Gronau, Q. F., Bergh, D. van den, & Wagenmakers, E.-J. (2018). Quantifying Support for the Null Hypothesis in Psychology: An Empirical Investigation: *Advances in Methods and Practices in Psychological Science*. <https://doi.org/10.1177/2515245918773742>
- Alain, C., Woods, D. L., & Ogawa, K. H. (1994). Brain indices of automatic pattern processing: *NeuroReport*, 6(1), 140–144. <https://doi.org/10.1097/00001756-199412300-00036>
- Bendixen, A. (2014). Predictability effects in auditory scene analysis: a review. *Frontiers in Neuroscience*, 8. <https://doi.org/10.3389/fnins.2014.00060>
- Bigdely-Shamlo, N., Mullen, T., Kothe, C., Su, K.-M., & Robbins, K. A. (2015). The PREP pipeline: standardized preprocessing for large-scale EEG analysis. *Frontiers in Neuroinformatics*, 9. <https://doi.org/10.3389/fninf.2015.00016>
- Brainard, D. H. (1997). The Psychophysics Toolbox. *Spatial Vision*, 10(4), 433–436. <https://doi.org/10.1163/156856897X00357>
- Bregman, A. (1990). *Auditory scene analysis : the perceptual organization of sound*. MIT Press.
- Brown, W. (1910). SOME EXPERIMENTAL RESULTS IN THE CORRELATION OF MENTAL ABILITIES1. *British Journal of Psychology*, 1904-1920, 3(3), 296–322. <https://doi.org/10.1111/j.2044-8295.1910.tb00207.x>
- Carpenter, B., Gelman, A., Hoffman, M. D., Lee, D., Goodrich, B., Betancourt, M., Brubaker, M.,

- Guo, J., Li, P., & Riddell, A. (2017). Stan: A Probabilistic Programming Language. *Journal of Statistical Software*, 76(1), 1–32. <https://doi.org/10.18637/jss.v076.i01>
- Cherry, E. C. (1953). Some Experiments on the Recognition of Speech, with One and with Two Ears. *The Journal of the Acoustical Society of America*, 25(5), 975–979. <https://doi.org/10.1121/1.1907229>
- de Cheveigné, A. (2020). ZapLine: A simple and effective method to remove power line artifacts. *NeuroImage*, 207, 116356. <https://doi.org/10.1016/j.neuroimage.2019.116356>
- de Cheveigné, A., & Nelken, I. (2019). Filters: When, Why, and How (Not) to Use Them. *Neuron*, 102(2), 280–293. <https://doi.org/10.1016/j.neuron.2019.02.039>
- Delorme, A., & Makeig, S. (2004). EEGLAB: an open source toolbox for analysis of single-trial EEG dynamics including independent component analysis. *Journal of Neuroscience Methods*, 134(1), 9–21. <https://doi.org/10.1016/j.jneumeth.2003.10.009>
- Goodman, S. (2008). A Dirty Dozen: Twelve P-Value Misconceptions. *Seminars in Hematology*, 45(3), 135–140. <https://doi.org/10.1053/j.seminhematol.2008.04.003>
- Gramfort, A. (2013). MEG and EEG data analysis with MNE-Python. *Frontiers in Neuroscience*, 7. <https://doi.org/10.3389/fnins.2013.00267>
- Hubbard, R., & Lindsay, R. M. (2008). Why P Values Are Not a Useful Measure of Evidence in Statistical Significance Testing: *Theory & Psychology*. <https://doi.org/10.1177/0959354307086923>
- Ioannidis, J. P. A. (2005). Why Most Published Research Findings Are False. *PLOS Medicine*, 2(8), e124. <https://doi.org/10.1371/journal.pmed.0020124>
- Jasny, B. R., Chin, G., Chong, L., & Vignieri, S. (2011). Again, and Again, and Again *Science*, 334(6060), 1225–1225. <https://doi.org/10.1126/science.334.6060.1225>
- Kassambara, A. (2020). *rstatix: Pipe-friendly framework for basic statistical tests* [Manual].

<https://CRAN.R-project.org/package=rstatix>

Kirk, R. E. (1996). Practical Significance: A Concept Whose Time Has Come. *Educational and Psychological Measurement*, 56(5), 746–759. <https://doi.org/10.1177/0013164496056005002>

Kleiner, M., Brainard, D., Pelli, D., Ingling, A., Murray, R., & Broussard, C. (2007). What's new in psychtoolbox-3. *Perception*, 36(14), 1–16.

<https://nyuscholars.nyu.edu/en/publications/whats-new-in-psychtoolbox-3>

Lance, C. E., Butts, M. M., & Michels, L. C. (2006). The Sources of Four Commonly Reported Cutoff Criteria: What Did They Really Say? *Organizational Research Methods*, 9(2), 202–220. <https://doi.org/10.1177/1094428105284919>

May, P. J. C., & Tiitinen, H. (2010). Mismatch negativity (MMN), the deviance-elicited auditory deflection, explained. *Psychophysiology*, 47(1), 66–122.

<https://doi.org/https://doi.org/10.1111/j.1469-8986.2009.00856.x>

Meehl, P. E. (1978). Theoretical risks and tabular asterisks: Sir Karl, Sir Ronald, and the slow progress of soft psychology. *Journal of Consulting and Clinical Psychology*, 46(4), 806–834. <https://doi.org/10.1037/0022-006X.46.4.806>

Mullen, T. R., Kothe, C. A. E., Chi, Y. M., Ojeda, A., Kerth, T., Makeig, S., Jung, T.-P., & Cauwenberghs, G. (2015). Real-time neuroimaging and cognitive monitoring using wearable dry EEG. *IEEE Transactions on Biomedical Engineering*, 62(11), 2553–2567.

<https://doi.org/10.1109/TBME.2015.2481482>

Nordby, H., Roth, W. T., & Pfefferbaum, A. (1988). Event-Related Potentials to Breaks in Sequences of Alternating Pitches or Interstimulus Intervals. *Psychophysiology*, 25(3), 262–268.

<https://doi.org/10.1111/j.1469-8986.1988.tb01239.x>

Nunnally, J., Jum, N., Bernstein, I. H., & Bernstein, I. (1994). *Psychometric Theory*. McGraw-Hill Companies, Incorporated.

Paavilainen, P. (2013). The mismatch-negativity (MMN) component of the auditory

- event-related potential to violations of abstract regularities: A review. *International Journal of Psychophysiology*, 88(2), 109–123. <https://doi.org/10.1016/j.ijpsycho.2013.03.015>
- Perrin, F., Pernier, J., Bertrand, O., & Echallier, J. F. (1989). Spherical splines for scalp potential and current density mapping. *Electroencephalography and Clinical Neurophysiology*, 72(2), 184–187. [https://doi.org/10.1016/0013-4694\(89\)90180-6](https://doi.org/10.1016/0013-4694(89)90180-6)
- Pion-Tonachini, L., Kreutz-Delgado, K., & Makeig, S. (2019). ICLabel: An automated electroencephalographic independent component classifier, dataset, and website. *NeuroImage*, 198, 181–197. <https://doi.org/10.1016/j.neuroimage.2019.05.026>
- Popper, K. (1935). *Logik der Forschung: Zur Erkenntnistheorie der Modernen Naturwissenschaft*. Springer Vienna.
- Rouder, J. N., Speckman, P. L., Sun, D., Morey, R. D., & Iverson, G. (2009). Bayesian t tests for accepting and rejecting the null hypothesis. *Psychonomic Bulletin & Review*, 16(2), 225–237. <https://doi.org/10.3758/PBR.16.2.225>
- Saarinen, J., Paavilainen, P., Schöger, E., Tervaniemi, M., & Näätänen, R. (1992). Representation of abstract attributes of auditory stimuli in the human brain: *NeuroReport*, 3(12), 1149–1151. <https://doi.org/10.1097/00001756-199212000-00030>
- Scharf, F., & Müller, D. (in prep). *Predictable changes within fast-paced sound sequences do not elicit the mismatch negativity: An in-class replication study*.
- Schmidt, S. (2009). Shall we Really do it Again? The Powerful Concept of Replication is Neglected in the Social Sciences: *Review of General Psychology*. <https://doi.org/10.1037/a0015108>
- Schröger, E., Tervaniemi, M., Wolff, C., & Näätänen, R. N. (1996). Preattentive periodicity detection in auditory patterns as governed by time and intensity information. *Cognitive Brain Research*, 4(2), 145–148. [https://doi.org/10.1016/0926-6410\(96\)00023-7](https://doi.org/10.1016/0926-6410(96)00023-7)
- Sellke, T., Bayarri, M. J., & Berger, J. O. (2001). Calibration of p Values for Testing Precise Null Hypotheses. *The American Statistician*, 55(1), 62–71.

<https://doi.org/10.1198/000313001300339950>

Spearman, C. (1910). Correlation calculated from faulty data. *British Journal of Psychology*, 3, 271–295.

Squires, N. K., Squires, K. C., & Hillyard, S. A. (1975). Two varieties of long-latency positive waves evoked by unpredictable auditory stimuli in man. *Electroencephalography and Clinical Neurophysiology*, 38(4), 387–401. [https://doi.org/10.1016/0013-4694\(75\)90263-1](https://doi.org/10.1016/0013-4694(75)90263-1)

Stan Development Team. (2020). *RStan: the R interface to Stan*. <http://mc-stan.org/>

Sussman, E., Ritter, W., & Vaughan, H. G. (1998). Predictability of stimulus deviance and the mismatch negativity: *NeuroReport*, 9(18), 4167–4170.
<https://doi.org/10.1097/00001756-199812210-00031>

Sussman, E. S., & Gumenyuk, V. (2005). Organization of sequential sounds in auditory memory: *NeuroReport*, 16(13), 1519–1523. <https://doi.org/10.1097/01.wnr.0000177002.35193.4c>

Wacongne, C., Labyt, E., van Wassenhove, V., Bekinschtein, T., Naccache, L., & Dehaene, S. (2011). Evidence for a hierarchy of predictions and prediction errors in human cortex. *Proceedings of the National Academy of Sciences of the United States of America*, 108(51), 20754–20759.
<https://doi.org/10.1073/pnas.1117807108>

Wagenmakers, E.-J. (2007). A practical solution to the pervasive problems of p values. *Psychonomic Bulletin & Review*, 14(5), 779–804. <https://doi.org/10.3758/BF03194105>

Wagenmakers, E.-J., Marsman, M., Jamil, T., Ly, A., Verhagen, J., Love, J., Selker, R., Gronau, Q. F., Šmíra, M., Epskamp, S., Matzke, D., Rouder, J. N., & Morey, R. D. (2018). Bayesian inference for psychology. Part I: Theoretical advantages and practical ramifications. *Psychonomic Bulletin & Review*, 25(1), 35–57. <https://doi.org/10.3758/s13423-017-1343-3>

Widmann, A., Schröger, E., & Maess, B. (2015). Digital filter design for electrophysiological data – a practical approach. *Journal of Neuroscience Methods*, 250, 34–46.
<https://doi.org/10.1016/j.jneumeth.2014.08.002>

Winkler, István. (2007). Interpreting the Mismatch Negativity. *Journal of Psychophysiology*, 21(3-4), 147–163. <https://doi.org/10.1027/0269-8803.21.34.147>

Winkler, Irene, Debener, S., Müller, K.-R., & Tangermann, M. (2015). On the influence of high-pass filtering on ICA-based artifact reduction in EEG-ERP. *2015 37th Annual International Conference of the IEEE Engineering in Medicine and Biology Society (EMBC)*, 4101–4105. <https://doi.org/10.1109/EMBC.2015.7319296>